ARTICLE IN PRESS

The Egyptian Journal of Remote Sensing and Space Sciences xxx (2018) xxx–xxx

HOSTED BY

ELSEVIER

Contents lists available at ScienceDirect

The Egyptian Journal of Remote Sensing and Space Sciences

journal homepage: www.sciencedirect.com

Research Paper

Sensitivity of the subspace method for land cover classification

Hasi Bagan [a,b,*], Huilong Li [c,*], Yonghui Yang [c], Wataru Takeuchi [d], Yoshiki Yamagata [b]

[a] Institute of Urban Studies, Shanghai Normal University, Shanghai 200234, China
[b] Center for Global Environmental Research, National Institute for Environmental Studies, 16-2 Onogawa, Tsukuba-City, Ibaraki 305-8506, Japan
[c] Key Laboratory of Agricultural Water Resources, Centre for Agricultural Resources Research, Institute of Genetics and Developmental Biology, Chinese Academy of Sciences, Shijiazhuang 050021, PR China
[d] Institute of Industrial Science, University of Tokyo, Meguro-ku, Tokyo 153-8505, Japan

ARTICLE INFO

Article history:
Received 13 June 2017
Revised 8 December 2017
Accepted 28 December 2017
Available online xxxx

Keywords:
Land cover
Cropland
Subspace method
Training sample size

ABSTRACT

The quality of a supervised classification map depends on the quality of the ground reference data and the classification method used. However, training samples for agriculture landscapes are often mixed with noise. Therefore, the classification of agriculture regions using remotely sensed data requires the use of classification methods with good generalization capabilities. In this study, the performance of the subspace method in land cover classification of a complex cropping mix area is explored. Landsat-5 thematic mapper (TM) data were used to classify 12 different land cover classes in the study area, located between Tianjin and Tangshan cities in northern China. We compared the classification maps obtained using the subspace method with those obtained using the self-organizing map neural network (SOM) and maximum likelihood classification (MLC) methods. The results of this comparative study confirm that the subspace method performed better than both the SOM and MLC methods. Furthermore, a comparison of the sensitivity of these methods to the reduction in the training sample size shows that the subspace method has a lower sensitivity to variations in the number of training pixels used than the other two methods. Our results demonstrate the ability of the subspace method to distinguish between different crop types over a large area. Moreover, the subspace method is less sensitive to small training sample sizes than the other two methods.

1. Introduction

Rapid population growth coupled with economic growth and urbanization has led to an increased demand for food and water supply in China. The rapid rate of urbanization in China has been at the expense of green space. Most of the urban expansion took place in areas that were suitable for urban land use, and these were mostly agricultural areas (Bagan and Yamagata, 2014). Accurate crop type mapping is required to manage the increasing pressure to feed the growing population despite the scarcity of water resources (Qi et al., 2012; Salmon et al., 2015).

Earth observation satellite data such as Landsat data allow the extraction of more detailed information on specific conditions in an area so as to identify major crop types. Remote sensing image classification is an important technique in image processing and can extract useful information, by identifying the spectral signatures of land cover types, for natural resources management. Various remote sensing image classification methods have been used for cropland mapping. These include the commonly used maximum likelihood classifiers (MLCs) (EL-Magd et al., 2003), neural networks (Bagan et al., 2005), support vector machines (SVM) (Mathur and Foody, 2008; Zheng et al., 2015), and knowledge-based systems, such as random forest classifiers (Rodriguez-Galiano et al., 2012) and decision tree classifiers (Liu et al., 2016). Recently, some progress has been made in land cover classification techniques such as the convolutional neural network model (Maggiori et al., 2017) and subspace classification method (Bagan and Yamagata, 2010; Qian et al., 2014; Sun et al., 2017a,b).

Peer review under responsibility of National Authority for Remote Sensing and Space Sciences.

* Corresponding authors at: Institute of Urban Studies, Shanghai Normal University, Shanghai 200234, China (H. Bagan). Key Laboratory of Agricultural Water Resources, Centre for Agricultural Resources Research, Institute of Genetics and Developmental Biology, Chinese Academy of Sciences, Shijiazhuang 050021, PR China (H. Li).

E-mail addresses: hasi.bagan@nies.go.jp (H. Bagan), hlongli@sjziam.ac.cn (H. Li), yonghui.yang@sjziam.ac.cn (Y. Yang), wataru@iis.u-tokyo.ac.jp (W. Takeuchi), yamagata@nies.go.jp (Y. Yamagata).

https://doi.org/10.1016/j.ejrs.2017.12.003
1110-9823/

The subspace method provides new opportunities for the efficient classification of remotely sensed data. This method is nonparametric or at most, semiparametric. It involves no probabilistic assumptions and is based entirely on the measurements of the feature space. In pattern recognition, the subspace method has been widely used for face and speech recognition (Hayashi, 2014). The subspace method classifies patterns as elements of a vector space, that is, each class is represented by a subspace spanned by a group of basis vectors, which can be obtained by principal component analysis (PCA).

Although the subspace method is a promising tool for land cover classification, there are two major limitations of this method that may discourage widespread adoption. First, previous studies have not investigated the effect of variations in the training sample size on the classifier performance of the subspace method. Second, the applicability of the subspace method in cropland mapping has not been fully established.

Ground reference data play a fundamental role in supervised image classification methods (Foody et al., 2016). The size and quality of the training sample used in a supervised classification method can have an impact on the accuracy of the resulting classification map (Ekambaram et al., 2016). As is often the case with remote sensing mapping activities, supervised classification methods also require a rather large amount of field reference data to ensure successful training of the supervised classifier. The collection of such an extensive and reliable ground reference data set is not feasible from an operational perspective due to time and cost constraints. Although many classification methods have been proposed, the statistical evaluation of the effect of reduced training sample sizes on the performance of their classifiers has not been carried out. Therefore, it is necessary to investigate the performance of supervised classification methods by using different training sample sizes. We have used the subspace method for the classification of a site with high crop diversity, located between the cities of Tianjin and Tangshan in the North China Plain, to test and demonstrate the full scope and capability of the subspace method and to overcome the two limitations mentioned earlier.

The purpose of this study is to investigate, implement, and test the subspace method for the classification of major crop types using Landsat-5 thematic mapper (TM) imagery. We also investigated the effect of reduced training sample size on classification performance. Furthermore, we compared the effectiveness of the subspace method in the classification of major crop types to that of the two other machine learning algorithms, that is, the self-organizing map neural network (SOM), which is being increasingly used for land cover mapping, and MLC, which is commonly used for land cover mapping.

2. Methodology

2.1. Study area

The study area is located between the cities of Tianjin and Tangshan in the North China Plain, and covers an area of about 3000 km^2 (Fig. 1). It is an area with a complex cropping mix, characterized by a flat topography and numerous rivers and ponds. It has an average altitude of 3 m above sea level. Farmland accounts for about 60% of the total land area. Staple crops in this region are wheat and maize. Winter wheat usually occupies the fields from the beginning of October to June, and maize is grown from mid-June to September. The other vegetation includes cotton, rice, vegetables, soybean, trees, and wetland plant species.

A large portion of China's food comes from the North China Plain. The agricultural sector is experiencing water scarcity, and thus this agriculturally important region suffers from frequent droughts (Lohmar et al., 2003). Therefore, precise cropland mapping of this region will have a significant impact on water use management, economic growth, and the livelihood of the region's population.

2.2. Data description

Landsat-5 TM images (provided by the USGS) acquired on September 4, 2005 (path 122 row 33) were used for land cover classification, since earlier studies reported that September was the optimal period for spectral separation between the main crops cultivated in this area (Bagan et al., 2005). Landsat-5 TM has 7 spectral bands with a radiometric resolution of 8 bit; 6 of these spectral bands have a spatial resolution of 30 m and the remaining has a spatial resolution of 120 m (thermal band). In this study, an image subset consisting of 1936 pixels × 1614 pixels was extracted from the TM imagery for analysis (Fig. 1). TM band 6 (thermal band) was included for its potential to assist in vegetation classification, and thus, band 6 is resampled to a spatial resolution of 30 m. Landsat scenes provided by the USGS have already been terrain corrected using ground control points and a digital elevation model (USGS, 2016). Atmospheric correction was considered unnecessary since it is often equivalent to subtracting a constant from all the pixels in each spectral band for a single date TM image and has little effect on the classification accuracy.

In order to gain a thorough understanding of the ground truth situation, two field surveys were conducted in the fall of 2005. The first field survey was conducted on August 7, 2005 by using a vehicle video image system, which was equipped with a digital camcorder, a GPS receiver with a horizontal accuracy of 10 m,

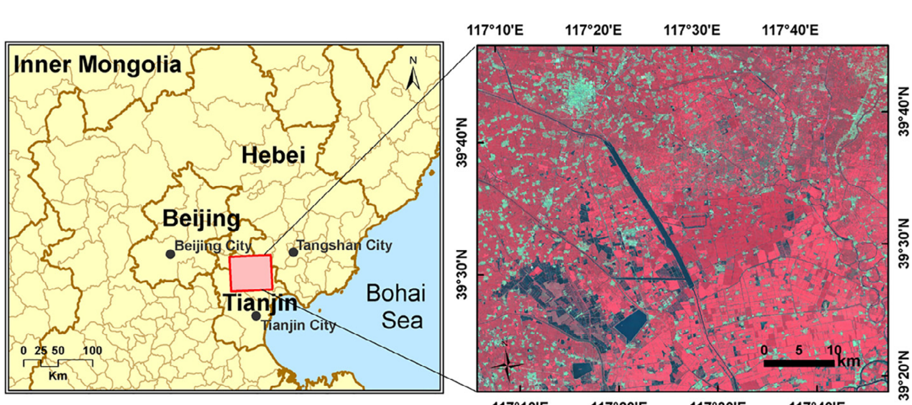

Fig. 1. Map of the study area located between Tianjin and Tangshan cities, North China (left) and the Landsat TM image (RGB = bands 4, 3, and 2) used in the study (right).

and a laptop. Land cover information was transferred from the digital camcorder and the GPS receiver to the laptop. The vehicle travelled 40 km along the main cropland, capturing 600 video frames of land cover with GPS coordinates. In addition, during the field surveys, photos were taken for different types of land cover along with GPS coordinates. In September 2005, another field survey was carried out to identify different crop types through on-site comparison of the ground truth of land cover with the recorded video images. These video frames were then used for manual digitization of the Landsat TM image to polygons in the laboratory.

2.3. Ground reference data collection

The main land cover classes in the study area are rice, summer maize, spring maize, cotton, soybean, vegetable land, harvested land, tree, reed, water body, residential, and other urban or built-up.

Ground reference sites for each mapping class and Landsat recording date were selected to accurately portray the spectral complexity and variability within each class. All the initially digitized ground reference sites were compared with the corresponding Landsat images to provide the correct interpretation of the time and date of image creation. As described above, ancillary images and GPS data sets were also used to support image interpretation and provide as much information as possible to help locate the ground reference sites. This ensured that all the selected samples could accurately represent a certain land cover class (Congalton and Green, 2009; Gómez et al., 2016). The selected reference sites were either polygonal or linear, and their locations were recorded using the ITT ENVI software package. The reference sites were then randomly divided into training and testing samples to ensure that they were spatially disjoint and to reduce any potential for correlation between the training data and test data. In total, 4533 training samples (pixels) and 1936 test samples were selected. The distribution of these samples in different land cover classes is given in Table 1.

2.4. Subspace classification methods

Subspace classification methods have been widely used to solve classification problems. The class-featuring information compression (CLAFIC) method and the multiple similarity method are classical subspace classification methods (Oja, 1983). These methods have been extended in various ways, such as the orthogonal subspace, mutual subspace, and kernel subspace methods (Washizawa, 2016). In the CLAFIC method, each class forms a lower dimensional subspace that is distinct from the subspace spanned by the other classes. The CLAFIC method and its classification criteria are as follows.

Table 1
Distribution of training and test samples in the different land cover classes of the study area.

Land cover class	Training samples	Testing samples
1. Tree	321	164
2. Reed	530	167
3. Rice	224	160
4. Summer maize	1060	214
5. Spring maize	442	177
6. Cotton	604	165
7. Soybean	174	135
8. Vegetable land	416	161
9. Harvested land	179	149
10. Residential	185	145
11. Other urban or built-up	146	120
12. Water body	252	179
Total	4533	1936

The orthonormal basis vectors of subspace U_i, which corresponds to land cover class $\omega^i (i = 1, 2, \cdots, c)$, are denoted by $u_1^i, u_2^i, \cdots, u_{p^i}^i$, where p^i is the dimensionality of the subspace. Any pixel x can be represented as a sum of two vectors, one belonging to the subspace U_i and the other orthogonal to it.

$$x = \hat{x}_i + \tilde{x}_i, \tag{1}$$

where $\hat{x}_i$ is the projection of pixel x on subspace U_i and $\tilde{x}_i$ is the vector orthogonal to subspace U_i. The orthogonal projection matrix on the subspace U_i can be computed from

$$P^i = \sum_{j=1}^{p^i} u_j^i u_j^{iT} \tag{2}$$

here u_j^{iT} is the transpose of basis vector u_j^i and P^i is a square symmetric matrix. The projection norm between pixel x and the subspace U_i can be measured from

$$\|\hat{x}\|^2 = \|P^i x\|^2 = x^T P^i x = \sum_{j=1}^{p^i} (x^T u_j^i)^2 \tag{3}$$

The classification rule is if

$$g(x, U_i) = \underset{i=1,2,\cdots,c}{\arg\max} \|P^i x\|^2 = \underset{i=1,2,\cdots,c}{\arg\max} \sum_{j=1}^{p^i} (x^T u_j^i)^2, \tag{4}$$

then x is classified into class ω^i.

One drawback of the CLAFIC method is that subspaces obtained for one class are not dependent on the subspaces obtained for the other classes. Therefore, subspaces obtained by the CLAFIC method may cause subspace overlay problems, which decrease the recognition rate. To avoid this drawback, the averaged learning subspace method (ALSM) was proposed for a more efficient separation of subspaces.

In the ALSM, CLAFIC is used to obtain the initial subspace and the subspace is rotated at each training iteration. To find the misclassified samples from the training sets, the following sets are calculated:

$$E_i = \{x | (x \in \omega_i) \cap (\text{but } x \text{ is classified to other class})\} \tag{5}$$

$$S_i = \{x | (x \notin \omega_i) \cap (\text{but x is classified to class } \omega_i)\} \tag{6}$$

Thus, the updated subspace for each class is obtained from the modified correlation matrix

$$U_i \leftarrow U_i + \alpha \sum_{x \in E_i} x x^T - \beta \sum_{x \in S_i} x x^T, \tag{7}$$

where the parameters α and β control the strength of the sets E_i and S_i, respectively. After the subspaces are updated, the sets E_i and S_i are updated again. Finally, the optimal subspaces for each class are obtained.

3. Results and discussion

3.1. Classification results

The proposed subspace method for multispectral classification was implemented using C++ programming language. The subspace dimensions were fixed at 3 and kept constant during the learning and classification process for each subspace (class) in the subspace method. The optimal values of the parameters α and β in Eq. (7) were fixed at 0.08, which was determined by an automatic optimization system (Bagan and Yamagata, 2010). After the parameter

Please cite this article in press as: Bagan, H., et al.. Egypt. J. Remote Sensing Space Sci. (2018), https://doi.org/10.1016/j.ejrs.2017.12.003

selection, the ALSM automatically determines the optimized subspaces for each class during the training phase. The constructed ALSM classifier was then applied to the multispectral TM data.

During the training stage of the subspace method, the classification accuracies for the training and testing data sets were determined by calculating the misclassification rate (error rate) under the respective iterations (Fig. 2). As shown in Fig. 2, the classification error rate for both the training and testing data sets decreased almost steadily with each learning iteration. For the training data set, it decreased from 14.8% to 4.1%, and for the testing data set, it decreased from 8.9% to 6.5%.

To compare the efficiency of the subspace classification method with that of the other methods, we classified the Landsat-5 TM images with 7 spectral bands (obtained on September 4, 2005) using the SOM and MLC methods with the same training and test data set. The parameters of the SOM neural network were set as follows: number of nodes in the input layer was set at 7; the competitive layer was a 20 × 20 two-dimensional set of neurons; the parameters of the neural network were set (based on testing) at a maximum iteration of 3000, an initial learning rate of 0.9, and a descending learning rate of 0.005. Learning vector quantization (LVQ) was applied to fine-tune the SOM weight vectors. The parameters of LVQ were set as follows: a maximum iteration of 1000, an initial learning rate of 0.0025, and a descending learning rate of 0.00001. After the training process was completed, land cover classification was performed using the SOM classifier. Details of the SOM classifier can be found in Bagan et al. (2008).

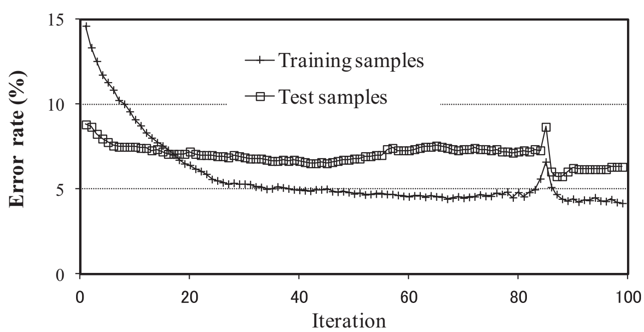

Fig. 2. Changes in the misclassification rate for the training and test samples of the subspace method with each training iteration.

The classification maps obtained using the MLC, SOM, and subspace methods are shown in Fig. 3(b)–(d). The accuracies of these classification maps were evaluated with the same test samples (Table 1).

The classification accuracy was assessed with the confusion matrix approach. Additionally, other indicators of classification accuracy, such as producer's accuracy, user's accuracies, overall classification accuracy, and kappa coefficient, were calculated.

The confusion matrix for the MLC, SOM, and subspace method is shown in Table 2–4, respectively. The classification accuracy of the subspace, SOM, and MLC method was 93.5%, 92.6%, and 91.7%, respectively. The subspace and SOM methods showed better efficiency than the MLC method. Kappa analysis was also performed; the kappa coefficient of the subspace, SOM, and MLC method is 0.93, 0.92, and 0.91, respectively. The subspace method had the best agreement between the classification map and the reference data. The subspace method showed good producer's and user's classification accuracies (Table 4) for almost all the land cover classes. The SOM and MLC methods, on the other hand, did not perform well in this regard and the accuracies were not consistent for the different land cover classes. For instance, the MLC method yielded high producer's accuracies for the reed, rice, summer maize, and cotton land cover classes, however, the user's accuracies were low for most of the land cover classes. Similarly, inconsistencies in the accuracies of the SOM method were observed, for instance in the classification of the tree and reed land cover classes (see Table 3). All the three methods showed high producer's accuracies for the rice, summer maize, and residential land cover classes. The user's accuracies of all the image classification methods were consistently high for the tree, harvested land, water body, and other urban built-up land cover classes.

Misclassification and spectral confusion of different land covers were considered to be caused by spectral similarities of different land covers. Therefore, there is high percentage of mixed pixels in the image data, for instance summer maize are often mixed up with trees in the so called agro-forestry system, and reed usually grows along the boundary of crop lands. A mixture of different vegetation

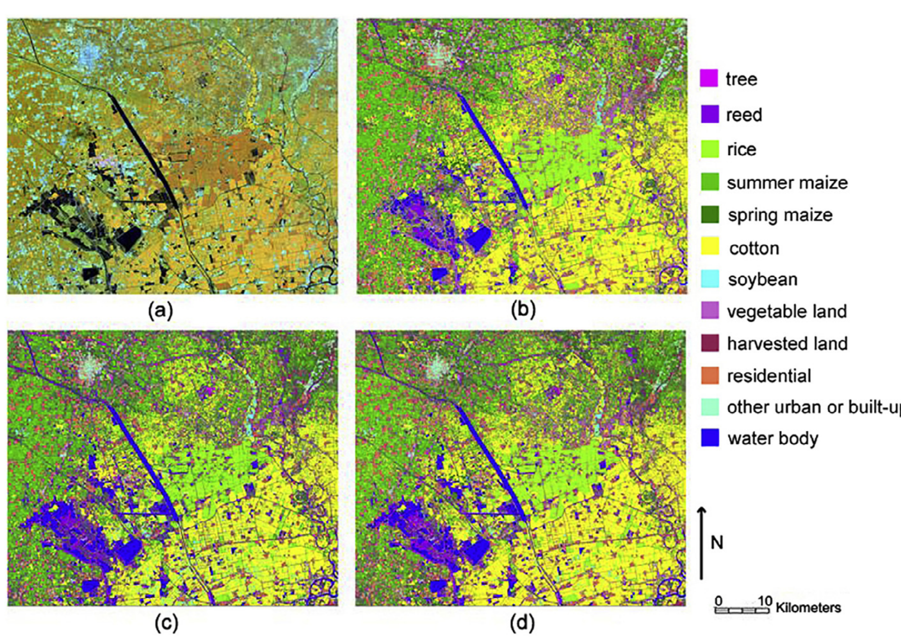

Fig. 3. (a) TM image subset (RGB = bands 4, 5, and 3) and classification maps generated by (b) the MLC method, (c) the SOM method, and (d) the subspace method.

Please cite this article in press as: Bagan, H., et al.. Egypt. J. Remote Sensing Space Sci. (2018), https://doi.org/10.1016/j.ejrs.2017.12.003

Table 2
Confusion matrix for the MLC method.

Class	1	2	3	4	5	6	7	8	9	10	11	12	Total	UA (%)
1	***111***	0	0	0	0	0	0	0	0	0	0	0	111	100
2	0	***165***	0	0	28	0	0	2	1	0	0	3	199	82.9
3	2	0	***160***	0	0	0	0	0	0	0	0	18	180	88.9
4	51	0	0	***214***	0	0	0	0	0	0	0	0	265	80.8
5	0	0	0	0	***139***	0	0	0	1	0	0	0	140	99.3
6	0	0	0	0	0	***164***	26	0	0	0	0	0	190	86.3
7	0	0	0	0	0	1	***109***	0	0	0	0	0	110	99.1
8	0	2	0	0	10	0	0	***159***	4	0	0	0	175	90.9
9	0	0	0	0	0	0	0	0	***140***	0	0	0	140	100
10	0	0	0	0	0	0	0	0	3	***145***	8	0	156	93.0
11	0	0	0	0	0	0	0	0	0	0	***112***	0	112	100
12	0	0	0	0	0	0	0	0	0	0	0	***158***	158	100
Total	164	167	160	214	177	165	135	161	149	145	120	179	1936	
PA (%)	67.7	98.8	100	100	78.5	99.4	80.7	98.8	94.0	100	93.3	88.3		

Overall classification accuracy: 91.74%; Kappa coefficient: 0.9096; UA = user's accuracy; PA = producer's accuracy.

Table 3
Confusion matrix for the SOM method.

Class	1	2	3	4	5	6	7	8	9	10	11	12	Total	UA (%)
1	***147***	0	0	0	0	0	0	1	0	0	0	0	148	99.3
2	0	***152***	0	0	26	0	0	12	2	0	0	0	192	79.2
3	4	0	***144***	0	0	0	0	0	0	0	0	0	148	97.3
4	13	0	16	***214***	0	0	0	0	0	0	0	0	243	88.1
5	0	15	0	0	***150***	0	0	13	0	0	0	0	178	84.3
6	0	0	0	0	0	***150***	14	0	0	0	0	0	164	91.5
7	0	0	0	0	0	15	***121***	0	0	0	0	0	136	89.0
8	0	0	0	0	1	0	0	***134***	0	0	1	0	136	98.5
9	0	0	0	0	0	0	0	1	***139***	0	0	0	140	99.3
10	0	0	0	0	0	0	0	0	8	***145***	2	0	155	93.6
11	0	0	0	0	0	0	0	0	0	0	***117***	0	117	100
12	0	0	0	0	0	0	0	0	0	0	0	***179***	179	100
Total	164	167	160	214	177	165	135	161	149	145	120	179	1936	
PA (%)	89.6	91.0	90	100	84.8	90.9	89.6	83.2	93.3	100	97.5	100		

Overall classification accuracy: 92.56%; Kappa coefficient: 0.9187; UA = user's accuracy; PA = producer's accuracy.

Table 4
Confusion matrix for the subspace method.

Class	1	2	3	4	5	6	7	8	9	10	11	12	Total	UA (%)
1	152	0	0	6	0	0	0	0	0	0	0	0	158	96.2
2	0	***155***	0	0	11	0	0	4	0	0	0	0	170	91.2
3	0	0	***160***	0	0	0	0	0	0	0	0	0	160	100
4	12	0	0	***206***	0	0	0	0	0	0	0	0	218	94.5
5	0	9	0	0	***160***	0	0	7	0	0	0	0	176	90.9
6	0	0	0	2	0	***138***	20	0	0	0	0	0	160	86.3
7	0	0	0	0	0	27	***115***	0	0	0	0	0	142	81.0
8	0	2	0	0	6	0	0	***146***	3	0	2	0	159	91.8
9	0	1	0	0	0	0	0	4	***141***	0	0	0	146	96.6
10	0	0	0	0	0	0	0	0	5	***144***	3	0	152	94.7
11	0	0	0	0	0	0	0	0	0	1	***115***	0	116	99.1
12	0	0	0	0	0	0	0	0	0	0	0	***179***	179	100
Total	164	167	160	214	177	165	135	161	149	145	120	179	1936	
PA (%)	92.7	92.8	100	96.3	90.4	83.6	85.2	90.7	94.6	99.3	95.8	100		

Overall classification accuracy: 93.54%; Kappa coefficient: 0.9294; UA = user's accuracy; PA = producer's accuracy.

causes difficulties in land cover classification. Fig. 4 shows the variation in the mean spectral values of different land covers at different Landsat TM spectral bands derived from the training samples. Spectral similarities are obvious between the tree and summer maize land cover classes and the cotton and soybean land cover classes.

3.2. Evaluation of the effect of reduced training set on classification accuracy

Supervised classification methods require a rather large amount of field reference data in order to ensure successful training of the supervised classifier. The size of the training data used in a supervised classification method can influence the accuracy of the resulting classification map. Thus, a statistical evaluation of the impact of training sample size reduction on the performance of the classification method is necessary.

Reduced training data sets, ranging from 10% to 90% (in a 10% interval) of the original training sample size, were derived to evaluate the sensitivity of the three classification methods to variations in the number of training pixels (Table 5). Each of training set was generated using a proportionate stratified random sampling method. The same original testing set was applied for the evaluation of the

Please cite this article in press as: Bagan, H., et al.. Egypt. J. Remote Sensing Space Sci. (2018), https://doi.org/10.1016/j.ejrs.2017.12.003

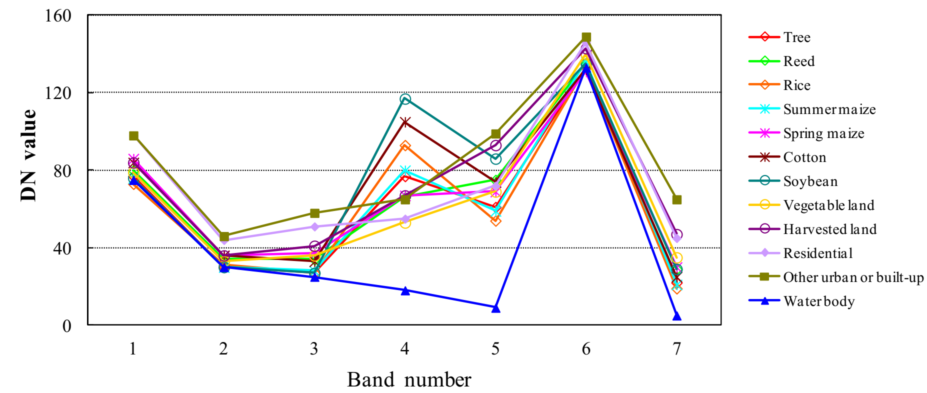

Fig. 4. Mean spectral values (DN: digital number) of different land cover classes in the study area.

Table 5
Classification accuracies of the MLC, SOM, and subspace methods with different training sample sizes.

Classifiers		Percentage of training set size (%)									
		10	20	30	40	50	60	70	80	90	100
MLC	Overall accuracy (%)	80.48	88.48	90.24	91.43	90.70	91.94	91.27	91.48	92.36	91.74
SOM	Overall accuracy (%)	90.08	91.74	91.22	91.12	91.43	91.53	90.91	91.94	91.79	92.56
subspace	Overall accuracy (%)	90.96	90.39	90.29	91.58	91.12	92.20	92.56	92.30	92.98	93.54

three classifiers. Comparison of the classification accuracies of the different classifiers using different sample sets is shown in Table 5.

For all the three classification methods, it was obvious that classification accuracy is positively related to training set size. For the MLC method, the difference between the classification accuracy achieved with the largest and smallest training sample size was 11.3%. Classification accuracies of the subspace and SOM method seemed to be less sensitive to reduction in training set size. For the subspace and SOM method, the difference between the classification accuracy achieved using the largest and smallest training sample size were only 3.3% and 2.5%, respectively. This may be because the MLC method is based on the assumption of normal or near normal spectral distribution for each class of interest. An equal prior probability among the classes is also assumed (Lillesand et al., 2008).

Fig. 5 shows the variation in the classification accuracies of the three classifiers with different training sample sizes. The MLC method needs a training data size that is at least 30% of the original training sample size to reach a relatively stable accuracy. However, the subspace and SOM method need a training sample size that is about 10% of the original training sample size to achieve stable classification accuracies. The results of our study highlight the advantages of the subspace method equal to or over the other classification methods, that is, it requires a relatively small training sample size for precise cropland mapping.

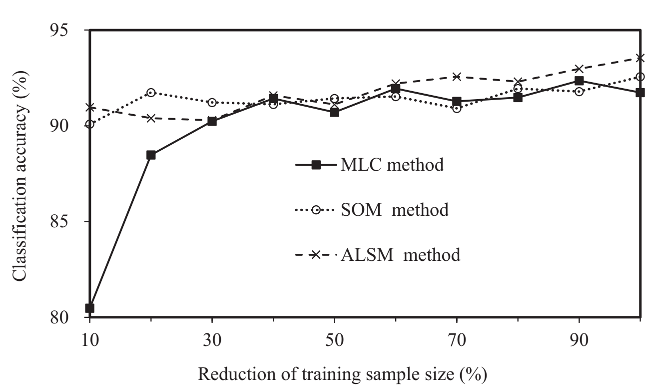

Fig. 5. Relationship between classification accuracy and the percentage reduction in the training sample size.

4. Conclusions

In this study, we used the subspace method for the identification of major crop types in an agricultural area of the North China Plain using multispectral remotely sensed data. The classification results of the Landsat TM data demonstrated that the subspace method was more effective than the SOM and MLC methods in terms of overall and individual crop classification accuracies. The advantages of the subspace method over the SOM and MLC methods include the need for fewer parameters and lower sensitivity to the reduction in the training sample size. Therefore, the proposed subspace method seems to be a promising alternative to the SOM method for crop type classification. It is worth mentioning that the performance of the subspace method is less dependent on the dimensionality of the input space unlike the MLC and SOM methods. Thus, the subspace method has a high potential for the classification of other types of remotely sensed data and time-series remotely sensed data. Although the performance of the subspace method in the present study was good, further research is required. This especially includes analyzing the influence of the parameters of the subspace method on its classification accuracy, and testing the capability of the subspace method in land cover classification of regions with entirely different crop types using other multispectral images.

Conflict of interest

The authors declare no conflict of interest regarding the publication of this paper.

Acknowledgements

This research was supported by the Environment Research and Technology Development Fund (S-10) of the Ministry of the Environment, Japan and supported by the NSFC (Grant No. 41771372).

References

Bagan, H., Yamagata, Y., 2010. Improved subspace classification method for multispectral remote sensing image classification. Photogramm. Eng. Remote Sens. 76 (11), 1239–1251.

Bagan, H., Yamagata, Y., 2014. Land-cover change analysis in 50 global cities by using a combination of Landsat data and analysis of grid cells. Environ. Res. Lett. 9 (6), 064015.

Bagan, H., Wang, Q., Watanabe, M., Yang, Y., Ma, J., 2005. Land cover classification from MODIS EVI times-series data using SOM neural network. Int. J. Remote Sens. 26, 4999–5012.

Bagan, H., Wang, Q., Watanabe, M., Kameyama, S., Bao, Y., 2008. Landcover classification using ASTER multi-band combinations based on wavelet fusion and SOM neural network. Photogramm. Eng. Remote Sens. 74, 333–342.

Congalton, R., Green, K., 2009. Assessing the Accuracy of Remotely Sensed Data: Principles and Practices; Mapping Science Series; CRC Press: Boca Raton. FL, USA.

Ekambaram, R., Fefilatyev, S., Shreve, M., Kramer, K., Hall, L.O., Goldgof, D.B., Kasturi, R., 2016. Active cleaning of label noise. Pattern Recogn. 51, 463–480.

EL-Magd, I.A., Tanton, T.W., 2003. Improvements in land use mapping for irrigated agriculture from satellite sensor data using a multi-stage maximum likelihood classification. Int. J. Remote Sens. 24, 4197–4206.

Foody, G.M., Pal, M., Rocchini, D., Garzon-Lopez, C.X., Bastin, L., 2016. The sensitivity of mapping methods to reference data quality: training supervised image classifications with imperfect reference data. ISPRS Int. J. Geo-Inf. 5 (11), 199.

Gómez, C., White, J.C., Wulder, M.A., 2016. Optical remotely sensed time series data for land cover classification: a Review. ISPRS J. Photogramm. Remote Sens. 116, 55–72.

Hayashi, K., 2014. Influence functions for a linear subspace method. Pattern Recogn. 47 (6), 2241–2254.

Lillesand, T., Kiefer, R.W., Chipman, J., 2008. Remote Sensing and Image Interpretation. Wiley, New York, p. 2008.

Liu, J., Huffman, T., Shang, J., Qian, B., Dong, T., Zhang, Y., 2016. Identifying major crop types in eastern Canada using a fuzzy decision tree classifier and phenological indicators derived from time series MODIS data. Can. J. Remote Sens. 42, 259–273.

Lohmar, B., Wang, J., Rozelle, S., Huang, J., Dawe, D., 2003. China's agricultural water policy reforms: increasing investment, resolving conflicts, and revising incentives. Agriculture Information Bulletin No. 782, Economic Research Service, US Department of Agriculture, Washington, DC, March 2003.

Maggiori, E., Tarabalka, Y., Charpiat, G., Alliez, P., 2017. Convolutional Neural Networks for Large-Scale Remote-Sensing Image Classification. IEEE Trans. Geosci. Remote Sens. 55 (2), 645–657.

Mathur, A., Foody, G.M., 2008. Crop classification by support vector machine with intelligently selected training data for an operational application. Int. J. Remote Sens. 29, 2227–2240.

Oja, E., 1983. Subspace Methods of Pattern Recognition. Research Studies Press and John Wiley & Sons, Letchworth, U.K..

Qi, X., Liu, L., Liu, Y., Yao, L., 2012. Risk assessment for sustainable food security in China according to integrated food security - taking Dongting Lake area for example. Environ. Monit. Assess. 185, 4855–4867.

Qian, T., Bagan, H., Kinoshita, T., Yamagata, Y., 2014. Spatial–temporal analyses of surface coal mining dominated land degradation in Holingol, Inner Mongolia. IEEE J. Selected Topics Appl. Earth Observ. Remote Sens. 7, 1675–1687.

Rodriguez-Galiano, V.F., Ghimire, B., Rogan, J., Chica-Olmo, M., Rigol-Sanchez, J.P., 2012. An assessment of the effectiveness of a random forest classifier for land-cover classification. ISPRS J. Photogramm. Remote Sens. 67, 93–104.

Salmon, J.M., Friedl, M.A., Frolking, S., Wisser, D., Douglas, E.M., 2015. Global rain-fed, irrigated, and paddy croplands: a new high resolution map derived from remote sensing, crop inventories and climate data. Int. J. Appl. Earth Observ. Geoinf. 38, 321–334.

Sun, W., Ma, J., Yang, G., Du, B., Zhang, L., 2017a. A Poisson nonnegative matrix factorization method with parameter subspace clustering constraint for endmember extraction in hyperspectral imagery. ISPRS J. Photogramm. Remote Sens. 128, 27–39.

Sun, W., Du, B., Xiong, S., 2017b. Quantifying sub-pixel surface water coverage in urban environments using low-albedo fraction from landsat imagery. Remote Sensing 9 (5), 428.

U.S. Geological Survey (USGS). (2016). Landsat Processing Details. Available at: http://landsat.usgs.gov/Landsat_Processing_Details.php (last accessed: 02 May 2017).

Washizawa, Y., 2016. Learning subspace classification using subset approximated kernel principal component analysis. IEICE Trans. Inf. Syst. 99 (5), 1353–1363.

Zheng, B., Myint, S.W., Thenkabail, P.S., Aggarwal, R.M., 2015. A support vector machine to identify irrigated crop types using time-series Landsat NDVI data. Int. J. Appl. Earth Observ. Geoinf. 34, 103–112.

Please cite this article in press as: Bagan, H., et al.. Egypt. J. Remote Sensing Space Sci. (2018), https://doi.org/10.1016/j.ejrs.2017.12.003